

Targeting naturally occurring epitope variants of hepatitis C virus with high-affinity T-cell receptors

Huajun Zhang,^{1†} Jianbing Zhang,² Lei Chen,² Zhiming Weng,² Ye Tian,¹ Haifeng Zhao,² Youjia Li,¹ Lin Chen,¹ Zhaoduan Liang,¹ Hongjun Zheng,² Wenzhuo Zhao,² Shi Zhong² and Yi Li^{1,2,*}

Abstract

Hepatitis C virus (HCV) readily establishes chronic infection, which is characterized by failure of virus-specific CD8⁺ T cells. HCV uses epitope mutation and T-cell exhaustion to escape from the host immune response. Previously, we engineered high-affinity T-cell receptors (HATs) targeting human immunodeficiency virus escape mutants. In this study, the affinity of a T-cell receptor specific for the HLA-A2-restricted HCV immunodominant epitope NS3 1406–1415 (KLVALGINAV) was improved from a K_D of 6.6 μ M to 40 pM. These HATs could also target HCV NS3 naturally occurring variants, including an escape variant vrt1 (KLVVLGINAV), with high affinities. The HATs can be used as high-affinity targeting molecules at the centre of the immune synapse for the HLA-restricted NS3 antigen. By fusing the HAT with a T-cell activation molecule, an anti-CD3 single-chain variable fragment, we constructed a molecule called high-affinity T-cell activation core (HATac), which can redirect functional CTLs possessing any specificity to recognize and kill cells presenting HCV NS3 antigens. This capability was verified with T2 cells loaded with prototype or variant peptides and HepG2 cells expressing the truncated NS3 prototype or variant proteins. The results indicate that HATac targeting the HLA-restricted NS3 antigen may provide a useful tool for circumventing immune escape mutants and T-cell exhaustion caused by HCV infection.

INTRODUCTION

Hepatitis C virus (HCV) is a global public health concern, with about 150 million people in the world chronically infected and more than 350 000 people estimated to die annually from HCV-related liver diseases. After infection, only a minority of patients can resolve spontaneously, whereas 75–85 % of those are unable to clear the virus, thus resulting in chronic infection that potentially leads to severe liver problems, including cirrhosis and liver cancer [1, 2]. The development of direct-acting antiviral (DAA) agents is a breakthrough in the treatment of chronic HCV infection. When used in combination with pegylated IFN and ribavirin, DAAs improve treatment efficacy compared to traditional dual therapy, and extra DAAs make IFN-free combination regimens possible [3]. However, a problem with DAAs is drug resistance [4, 5], and more resistant virus strains may appear as these DAAs are more widely used. Hence, it is desirable to explore novel strategies for treating HCV infection.

Viral-specific T-cell response is believed to play a major role in determining the outcome of HCV infection [6]. Especially in the early stage of infection, the vigour of T-cell response may be a critical determinant of disease resolution and infection control [7]. Chronic HCV infection is characterized by the failure of the viral-specific CD8⁺ T-cell response [8]. Two mechanisms lead to the failure of this response. Accumulating evidence has shed light on the first mechanism, in which HCV can escape the host immune response by generating amino acid mutations in its antigen epitopes [9–13]. For example, Cox *et al.* [9] identified escape mutations in multiple CTL epitopes from seven persistently infected individuals. In another study in which two patients were accidentally infected from a single source but developed either a persistent or resolved infection, an escape mutation was identified from the patient with persistent infection [11]. The escape mutation (named as 'vrt1' in this study) occurred in the HLA-A2-restricted immunodominant epitope NS3 1406–1415 (NS3-

Received 12 August 2016; Accepted 10 November 2016

Author affiliations: ¹State Key Lab of Respiratory Disease, Guangzhou Institutes of Biomedicine and Health, Chinese Academy of Sciences, Guangzhou, PR China; ²XiangXue Life Sciences Research Center, XiangXue Pharmaceutical Co. Ltd, Guangzhou, PR China.

*Correspondence: Yi Li, li_yi@gjhb.ac.cn

Keywords: epitope mutation; T cell exhaustion; pHLA; cytotoxic killing; anti-CD3.

Abbreviations: CDR, complementarity-determining region; CMV, cytomegalovirus; cSMAC, central supramolecular activation cluster; DAA, direct-acting antiviral agent; HAT, high-affinity T-cell receptor; HATac, high-affinity T-cell activation core; HCV, hepatitis C virus; HIV, human immunodeficiency virus; IBs, inclusion bodies; PBMS, PBS containing 5 % skim milk; PBST, PBS containing 0.05 % Tween 20; pHLA, peptide-HLA; pHLA_{bio}, biotinylated peptide-HLA; pt, prototype; scFv, single-chain variable fragment; SPR, surface plasmon resonance; TCR, T-cell receptor.

†Present address: Wuhan Institute of Virology, Chinese Academy of Sciences, Wuhan, PR China.

Three supplementary figures are available with the online Supplementary Material.

1406), in which the alanine at the fourth position in the prototype (pt) sequence, KLVALGINAV, was replaced by valine. However, no mutation was observed from the resolved individuals in either study.

The other mechanism for persistent infection is T-cell exhaustion [14], which is a state of T-cell dysfunction that arises during many chronic infections and cancers, whereby antigens can be present for many years [15]. With the expression of inhibitory receptors on their cell surface [16], HCV-specific CD8⁺ T cells can be detected in PBMCs from chronically infected patients but are dysfunctional in proliferation, cytokine production and cytolytic activity [17, 18]. T-cell exhaustion appears to be antigen (HCV) specific, as non-HCV-specific CD8⁺ T cells from chronic HCV patients are fully functional; for example, cytomegalovirus (CMV)-specific CD8⁺ T cells of patients responded well to stimulation of the CMV peptide antigen [18]. Thus, it appears that there is no shortage of CTLs for eliminating viral infected cells; the question is how to promote functionally capable CD8⁺ T cells to target HCV-infected cells and resolve the problem of T-cell exhaustion.

To tackle the two mechanisms of HCV escaping immune control in patients, we propose a way to enhance the capability of T cells to recognize HCV-infected cells, including those with escape mutants, and ultimately cure HCV infection. One of the fundamental elements in T-cell recognition and activation is immunological synapse, which is assembled between a T cell and an antigen-presenting cell with the core molecule pair formation between a T-cell receptor (TCR) and a peptide–HLA (pHLA). Observation of the centre of the immunological synapse with confocal microscopy showed that TCR microclusters, which interact with pHLA molecules, are the fundamental structures associated with T-cell signalling [19]. The optimal agonist signals can only be generated when each TCR microcluster encounters multiple pHLAs [20], and normally, each cell can present hundreds or thousands of pHLAs. This finding indicates that a low number of pHLAs are not sufficient to trigger the T-cell response via a TCR microcluster. The reason may be that the TCR binding to the pHLA is naturally characterized as

low affinity with K_D over 1 μ M. We propose that if the binding strength of a TCR toward pHLA is enhanced, fewer copy numbers of pHLAs may be required to activate a T cell. It has been verified that high-affinity TCRs (HATs) [21] can direct a T cell to kill a cancer cell displaying only 50 copies of relevant pHLAs [22], whereas wild-type or low-affinity TCRs fail to produce similar results.

The idea of using affinity-enhanced TCRs to capture viral escape mutants has been tested with T cells transduced with the gene of HATs recognizing a human immunodeficiency virus (HIV) gag epitope [23]. Here, we investigate whether affinity-enhanced HCV-specific TCRs can be used to eliminate naturally occurring variants of HCV. Instead of using transduced T cells with HATs, we use soluble bi-functional molecules to direct fully functional CTLs possessing any specificity to control HCV escape mutants. Using a TCR against HLA-A2-restricted antigen NS3-1406 [24], we applied phage display libraries to generate three HATs with K_D ranging from nano- to pico-molar. To investigate whether the HATs could be used to target and lead to cytotoxicity against HCV-infected cells, we constructed a molecule named high-affinity T-cell activation core (HATac), which was a fusion protein with one HAT-containing arm to tightly bind the target cells presenting HLA-restricted epitopes, and another antibody single-chain variable fragment (scFv) arm (aCD3) to bind CD3 at the centre of the immune synapse. In comparison with the natural immune synapse, in which the TCR-rich central supramolecular activation cluster (cSMAC) is formed by the interaction between multiple copies of wild-type TCRs (low affinity) and pHLAs of the target cells [19], a HATac, with HAT to the pHLA, acted as a core to build a new cSMAC and trigger T-cell activation (Fig. 1). The recognition of NS3-1406 and various variants by the HAT was extensively evaluated by surface plasmon resonance (SPR) and cytotoxic assay with peptide-loaded T2 cells and antigen-expressing HepG2 cells. Our results demonstrated that the HATs can recognize NS3-1406 variants with high affinities, and the variation in affinities correlated with the phylogenetic distance. The results also demonstrated that HATacs can redirect CTLs

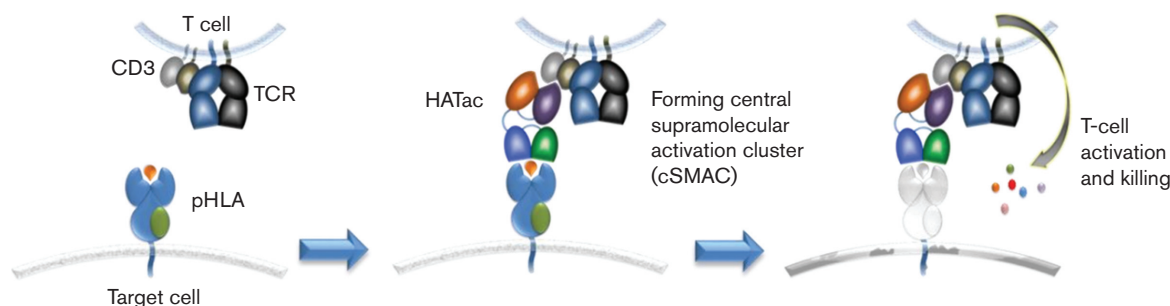


Fig. 1. Action of the HATac. The target cell, such as an HCV-infected cell, is bound by HAT fused with an anti-CD3 scFv partner that can bind to T cells possessing any specificity, for example, CMV-specific CD8⁺ T cells for overcoming HCV-specific T-cell exhaustion. Such interaction might form a stable cSMAC, which would result in CMV-specific T-cell activation to kill the HCV-infected target cell.

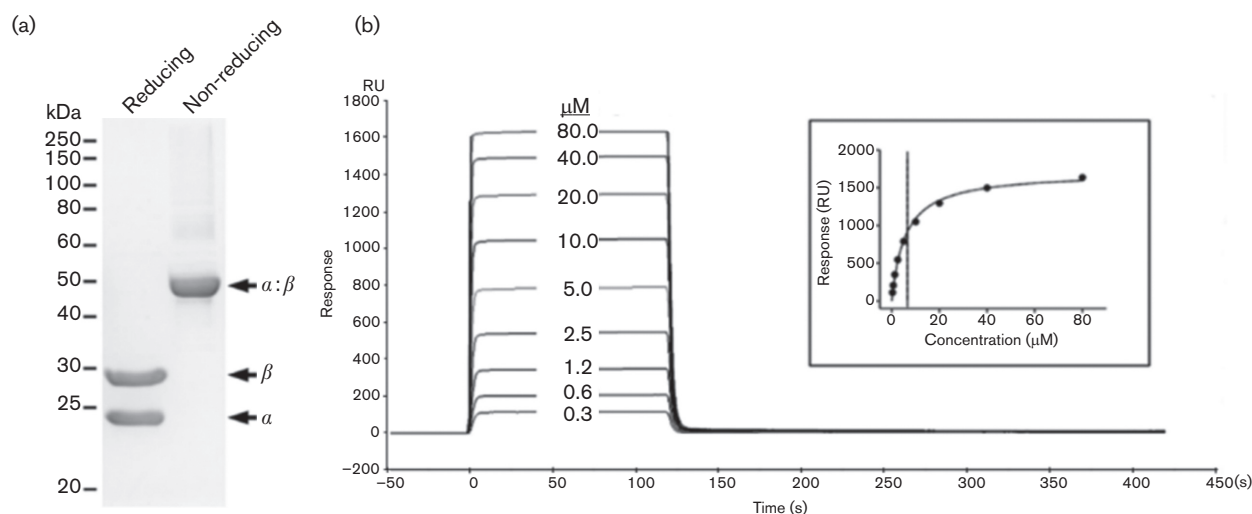


Fig. 2. Refolding and purification of wild-type TCR and the affinity measurement. TCR α and β chains were expressed in *Escherichia coli* BL21(DE3) as inclusion bodies. Soluble TCR was refolded *in vitro*, dialysed and purified with anion exchange chromatography. Purified TCR was analysed with reducing and non-reducing SDS-PAGE (a). CM5 BIAcore chips were coated with streptavidin using amine coupling, and then biotinylated pt NS3-1406 pHLA A0201 (pHLA-pt-bio) was captured on the active channel. Different concentrations of soluble TCR were injected sequentially through the reference and active channels with multi-cycle kinetics (b). The insert shows the non-linear fit of the Langmuir binding isotherm. The affinity (K_D) was determined to be 6.6 μ M using global fitting.

with different specificities to kill cells expressing closely related variant antigens. Thus, the present study presents a good method to tackle naturally occurring T cell epitope variants and T-cell exhaustion, and may provide a novel strategy for viral infection control.

RESULTS

Expression of wild-type TCR and affinity maturation

HLA-A2-restricted NS3-1406-specific CD8⁺ T cells and TCRs were generated as previously described by others [24, 25]. To analyse the affinity of the TCR against its cognate antigen, the soluble TCR heterodimer was produced by *in vitro* refolding and purification as described by Boulter *et al.* [26], with yields of 15–20% (Fig. 2a). Different concentrations of TCRs were injected through BIAcore chips captured with biotinylated pHLA (pHLA_{bio}) using multi-cycle kinetics on BIAcore T200 (Fig. S1, available in the online Supplementary Material). The K_D , the equilibrium dissociation constant between the TCR and the pHLA, was determined to be 6.6 μ M using global

fitting (Fig. 2b), which was in the typical range found in wild-type TCR against viral antigens [27].

To improve the affinity of the HCV-specific TCR, we constructed phage display libraries containing degenerated complementarity-determining regions (CDRs) of the TCR α and β chains, respectively. We identified two high-affinity mutant sequences from the CDR1 α library, one sequence from the CDR1 β library, and another two sequences from the CDR3 β library (Table 1). As published previously [21], mutant sequences from individual CDR libraries were assembled to achieve combined HAT mutants. The HAT mutant heterodimers were mixtures of different TCR α and β proteins, whereas the biotinylated heterodimer was made through the fusion of a biotin tag to β chains. The successfully prepared HAT heterodimers were immobilized on streptavidin-coated BIAcore chips to determine their binding affinities to pHLA-pt. The single CDR3 β HAT mutant had a K_D of 2 nM, whereas the combined HAT mutants of CDR1 α +CDR3 β or CDR1 α +CDR1 β +CDR3 β had a K_D of 140 or 40 pM, respectively (Table 1).

Table 1. HATs from phage display selection

TCR	α Chain		β Chain		K_D for pHLA-wt
	CDR1	CDR3	CDR1	CDR3	
wt	TSESDYY	AYGEDDKII	MGHDK	ASRRGPYEQY	6.6 μ M
HAT-2nMSLLV	2 nM
HAT-140pM	...E.ISA.L..	140 pM
HAT-40pM	...N.IY..SLLV	40 pM

Table 2. Recognition of NS3-1406 pHLA-vrts by HATs

pHLA	HAT-40pM			HAT-140pM			HAT-2nM			Sequences*
	k_a ($M^{-1}s^{-1}$)	k_d (s^{-1})	K_D (M)	k_a ($M^{-1}s^{-1}$)	k_d (s^{-1})	K_D (M)	k_a ($M^{-1}s^{-1}$)	k_d (s^{-1})	K_D (M)	
pt	2.7e+05	1.1e-05	4.0e-11	2.9e+05	4.1e-05	1.4e-10	3.2e+05	6.6e-04	2.1e-09	KLVALGINAV
VRT1	3.8e+05	6.3e-04	1.7e-09	4.2e+05	5.2e-04	1.2e-09	4.7e+05	1.1e-01	2.4e-07	KLVLGINAV
VRT2	2.8e+05	2.2e-04	7.8e-10	4.4e+05	3.8e-03	8.6e-09	4.1e+05	2.7e-02	6.6e-08	KLKSLGINAV
VRT3	6.6e+05	1.8e-03	2.7e-09	9.9e+05	5.3e-02	5.4e-08	8.5e+05	1.5e-01	1.8e-07	KLKSLGINAV
VRT4	2.8e+05	2.8e-03	1.0e-08	1.5e+05	5.9e-02	3.9e-07	2.9e+05	1.0e-01	3.6e-07	QLTSLGINAV
VRT5	2.9e+05	6.6e-03	2.3e-08	2.2e+05	1.4e-01	6.4e-07	4.2e+05	4.8e-01	1.1e-06	QLSSGINAV
VRT6	1.0e+04	4.2e-03	4.1e-07	5.1e+03	5.8e-02	1.1e-05	4.1e+03	5.4e-02	1.3e-05	QLRTGINAV
VRT7	4.1e+03	4.1e-03	1.0e-06	1.3e+03	3.7e-02	2.8e-05	1.4e+03	2.9e-02	2.1e-05	QLRSLGINAV
VRT8	9.0e+02	4.0e-03	4.4e-06	3.1e+02	2.5e-02	7.8e-05	2.3e+02	1.4e-02	6.0e-05	ALRGMGVNAV

*The varied residues are in bold letters.

Recognition of NS3-1406 variants by HATs

We found large amount of HCV sequence data from public HCV databases. To analyse the variants of NS3-1406, we collected 188 full-length HCV polyprotein sequences from GenBank in March 2014. Retrieving NS3-1406 epitope from these polyproteins resulted in 57 variants of NS3-1406, with some variants appearing multiple times. A maximum-likelihood phylogenetic tree was reconstituted for these decapeptides including the most pt-like variant KLVLGINAV (VRT1), which was reported to be an immune escape mutant [9, 11]. As shown in Fig. S2 and Table 2, the HLA anchor residues at positions 2 and 10 were highly conserved for leucine and valine, respectively, and only one strain (less than 0.6%) had the second position mutated to phenylalanine. The results of analysing these decapeptides from HCV polyproteins indicated that the mutations mainly occurred at the N-terminal half of the peptide from the third to the fifth residues. However, the first residue of the epitope was mainly glutamine found in 24 strains, followed by lysine in 20 strains, alanine in 13 strains and arginine or threonine in 1 strain. Starting from the C-terminal half of the peptide epitope, position 6 was strictly conserved for glycine and position 9 for alanine. Although position 7 was highly conserved for branched-chain amino acids (valine, leucine or isoleucine), position 8 was almost always asparagine, with less than 2% of strains having threonine and less than 1% having histidine. On the basis of natural viral mutation frequency, we prepared pHLA complexes of eight mutant peptides (pHLA-VRT1-8) and the pt peptide (pHLA-pt) for the investigation of HAT capabilities to target naturally occurring variants.

The recognition of pHLA-vrts by the three HATs was determined and is shown in Table 2 and Fig. 3. Interestingly, the three HATs recognized pHLA-vrts with decreasing affinities that primarily correlated with the phylogenetic distances of the mutant peptides relative to the pt peptide, with the exceptions of HAT-40pM and HAT-2nM, which recognized pHLA-VRT1 more weakly than pHLA-VRT2. None of the eight pHLA-vrts showed stronger binding with HATs than pHLA-pt, indicating that all three HATs were relatively specific.

For each individual antigen peptide, the three HATs bound pHLA-vrts with similar association rate constants (k_a), which varied by less than fourfold, but the dissociation rate constants (k_d) changed by more than 100-fold. For instance, pHLA-VRT1 was bound by HAT-40pM, HAT-140pM and HAT-2nM with a k_a of $(4.2 \pm 0.4) \times 10^5$ ($M^{-1}s^{-1}$), but their k_d values differed by more than 200-fold: 6.3×10^{-4} ($M^{-1}s^{-1}$), 5.2×10^{-4} ($M^{-1}s^{-1}$) and 1.1×10^{-1} ($M^{-1}s^{-1}$), respectively. Data for the binding of each HAT to different pHLAs showed that the k_a values varied within a limited range between 1.5×10^5 ($M^{-1}s^{-1}$) and 9.9×10^5 ($M^{-1}s^{-1}$) for pHLA-pt and pHLA-VRT1-5 and were at least 10 times higher than those for pHLA-VRT6-8, which ranged between 2.3×10^2 ($M^{-1}s^{-1}$) and 1.0×10^4 ($M^{-1}s^{-1}$). However, the k_d data were more complicated. In the case of HAT-40pM, in

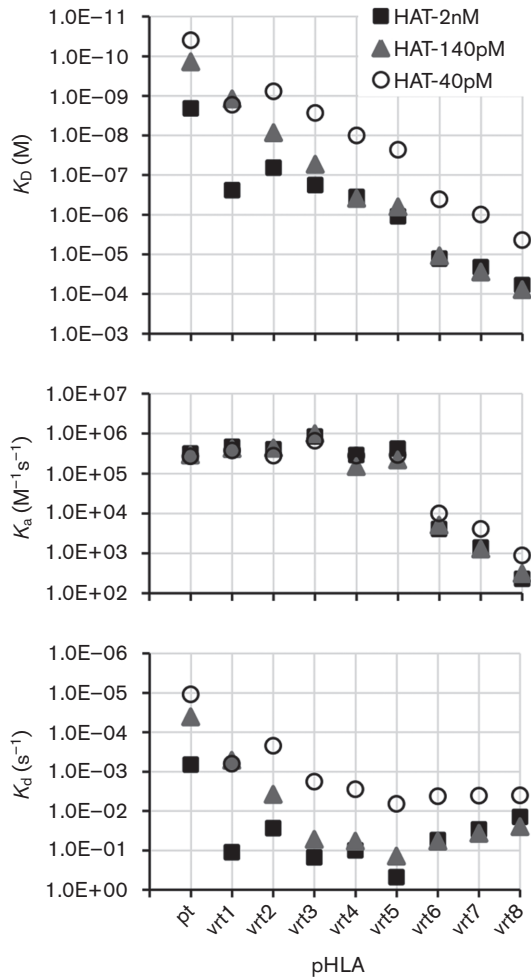


Fig. 3. Recognition of pHLA-vrts by HATs. Biotinylated HATs were immobilized on streptavidin-coated CM5 BIAcore chips, and pHLA-vrts were injected at various concentrations with single-cycle kinetics and also run as a negative control in the same setting to get the blank signals. The kinetic constants k_a , k_d and K_D were determined using BIAcore T200 evaluation software with a 1 : 1 binding model.

which the k_d values varied from 1.1×10^{-5} (s^{-1}) for pHLA-pt to 6.6×10^{-3} (s^{-1}) for pHLA-vrt5, there was almost no change for pHLA-vrt6-8, with k_d values of around $(4.1 \pm 0.1) \times 10^{-3}$ (s^{-1}). Moreover, the k_d values of HAT-140pM and HAT-2nM changed from 4.1×10^{-5} (s^{-1}) for HAT-140pM binding to pHLA-pt to 4.8×10^{-1} (s^{-1}) for HAT-2nM binding to pHLA-vrt5. In contrast, both HATs bound pHLA-vrt6-8 without significant variation in k_d values at around $(3.4 \pm 2.4) \times 10^{-2}$ (s^{-1}). In general, the affinities of the binding of the three HATs to pHLA-vrts closely correlated with the number of point mutations in the epitopes, in which more point mutations resulted in weaker binding.

Cytotoxic activity mediated by HATacs to peptide-loaded T2 cells

To direct CTLs for killing analysis, HATacs were constructed by fusing aCD3 (UCHT1) to the N-termini of β

chains of HAT-2nM, HAT-140pM and HAT-40pM by a GGGGS linker and by refolding with corresponding α chains (Figs 1 and S3). T cells can be activated by HATacs once mixed with cells presenting NS3-1406 peptides with HLA-A2. Activated T cells elicited multiple effector functions, including degranulation and the production of perforin and multiple cytokines. We detected IFN- γ and IL-2 release in the culture media of T2 cells loaded with 2×10^{-6} M pt peptide. Both IFN- γ and IL-2 were released in a HATac concentration-dependent manner (Fig. 4a). There was no difference in IFN- γ release among the three HATacs used, but HATac-2nM elicited less IL-2 than HATac-140pM and HATac-40pM. To investigate the redirected killing by T cells irrespective of their original specificity, we tested the activity of HATacs to direct CD8⁺ T cells to lyse T2 cells loaded with different amounts of NS3-1406 peptide. T2 cells were loaded with serial 10-fold diluted NS3-1406 pt peptide ranging from 2×10^{-6} M to 2×10^{-9} M and then co-cultured with expanded CD8⁺ T cells and the presence of HATacs at various concentrations. As shown in Fig. 4(b), the presence of 2×10^{-6} M pt peptide resulted in no difference in cell lysis between the three HATacs of HATac-2nM, HATac-140pM and HATac-40pM at all concentrations. With the presence of 2×10^{-7} M pt peptide, HATac-2nM did not mediate detectable lysis, whereas HATac-140pM-activated CD8⁺ T cells did lyse the cells to a marginally lower degree than that with HATac-40pM. Moreover, when the pt peptide was diluted to 2×10^{-8} M, only HATac-40pM showed 22 and 14 % specific lysis at the concentrations of 1 and 0.1 nM, respectively, and no significant lysis of T2 cells was detected for all HATacs when the cells were loaded with 2×10^{-9} M pt peptides. These results indicated that the activity to mediate specific lysis was closely related to both the affinity of HATs and the concentration of peptides used for loading the cells.

When the specific lysis effect on T2 cells was measured for NS3-1406 mutant peptides at the concentration of 2×10^{-6} M, T2 cells loaded with vrt1-5 could be lysed by CD8⁺ T cells activated with HATac-2nM, HATac-140pM or HATac-40pM, but not the cells loaded with vrt6-8 and the negative control peptide NS3-1073 (Fig. 5). In general, for an individual HATac or peptide, the higher the affinity of the TCRs, the greater the percentage of specific lysis to T2 cells loaded with the peptides, indicating that the HATac function of mediating specific lysis was closely related to the affinities of the TCRs.

Cytotoxic activity mediated by HATacs to epitope-expressing HepG2 cells

A previous study suggested that HIV-1 immune escape might be controlled by CD8⁺ T cells expressing an affinity-enhanced TCR specific for a pHLA-gag antigen [23]. Similarly to gag-specific TCR-transduced T cells, soluble HATacs could direct lysis to a group of HepG2 cells presenting escape mutants. To establish cell lines that expressed NS3 antigen endogenously and presented NS3-1406 epitopes, we transduced the HLA-A2-positive human hepatoma

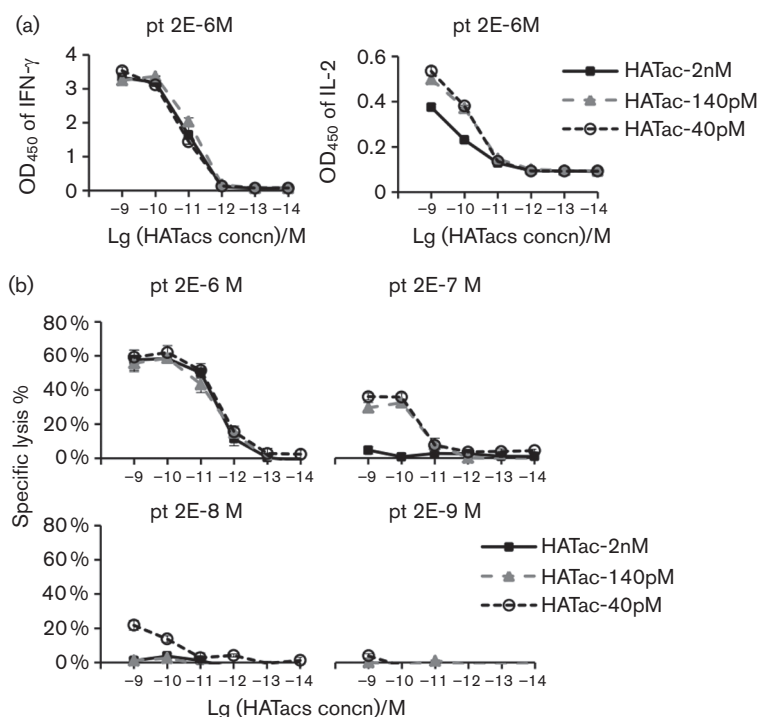


Fig. 4. Cytokine release and cytotoxicity assay with T2 cells loaded with pt peptide. (a) T2 cells were loaded with 2×10^{-6} M pt peptides for 2 h and then incubated with expanded CD8⁺ T cells in the presence of HATacs at the indicated concentrations; 20 h later, IFN- γ and IL-2 released in the medium were detected with ELISA. (b) T2 cells were loaded with pt peptide from 2×10^{-6} M to 2×10^{-9} M for 2 h and then incubated with CD8⁺ T cells as above. The specific lysis was determined with a CytoTox 96 Non-Radioactive Cytotoxicity Assay (Promega), which is based on lactatedehydrogenase (LDH) release. $n=3$.

cell line HepG2 with lentiviral vectors encoding the partial NS3 genes (amino acids 1353–1465) fused with EGFP, and the stably expressing cells were sorted with flow cytometry. These cell lines were co-cultured with CD8⁺ T cells and HATacs at concentrations of 1×10^{-9} M, 1×10^{-10} M and 1×10^{-11} M, respectively. The IFN- γ secretion of CD8⁺ T cells in the media was quantified by ELISA. As shown in Fig. 6(a), IFN- γ was released from the CD8⁺ T cells co-cultured with HepG2-pt and HepG2-vrt1-5 in a manner related to the affinities and doses of HATacs, but no significant IFN- γ release was detected for HepG2-vrt6-8 co-cultured with the CD8⁺ T cells. The specific lysis was also measured separately for each cell line (Fig. 6b). HATac-40pM at 1×10^{-11} M mediated significant lysis to HepG2-pt and HepG2-vrt1-3 and minimum lysis to HepG2-vrt4-5. Significant lysis was observed for HATac-140pM at 1×10^{-9} M and 1×10^{-10} M but not at 1×10^{-11} M, whereas HATac-2nM only mediated significant lysis to HepG2-pt and HepG2-vrt1-4 at 1×10^{-9} M. Consistent with the assay containing peptide-loaded T2 cells, no HATacs mediated specific lysis of HepG2-vrt6-8.

DISCUSSION

The mechanisms underlying chronic infection with HCV are the generation of viral escape mutants and viral-specific

T-cell exhaustion. As recently reviewed by Timm and Walker [28], the CD8⁺ T-cell response shapes viral intra- and inter-host evolution, and in turn, HCV sequence diversity influences the quality of the CD8⁺ T-cell response and thus infection outcome. Epitope mutation was found to lead to a markedly reduced CD8⁺ T cell response. Compared to NS3-1406 pt, the mutation (KLVAMGINAV) was reported to elicit half of the IFN- γ CD8⁺ T-cell response [9], whereas vrt1 (KLVV \underline{L} GINAV) failed to elicit a peptide-specific response [7, 11]. Redirected by affinity-improved TCR and anti-CD3 scFv, functional non-specific CTL can recognize and kill cells presenting the mutated epitopes or HCV variants, which tackles both viral escape mutations and viral-specific T-cell exhaustion simultaneously.

In addition to escape mutations, HCV has broad range of genotypes. The conserved epitope NS3-1406 varies between the genotypes [29]. Among these variants, an epitope of genotype 1b variant (KLSALGLNAV) showed superior immunogenicity to stimulated CD8⁺ T cells, with relative broad cross-reactivity recognizing several NS3-1406 epitope variants [30], including cross-reactive CD8⁺ T cells against genotype 1a variant (KLVALGINAV), which was used to generate the starting TCR for the current study. In Ziegler *et al.*'s study [30], the epitope of genotype 1a variant (KLVALGINAV) could only stimulate no or little cross-

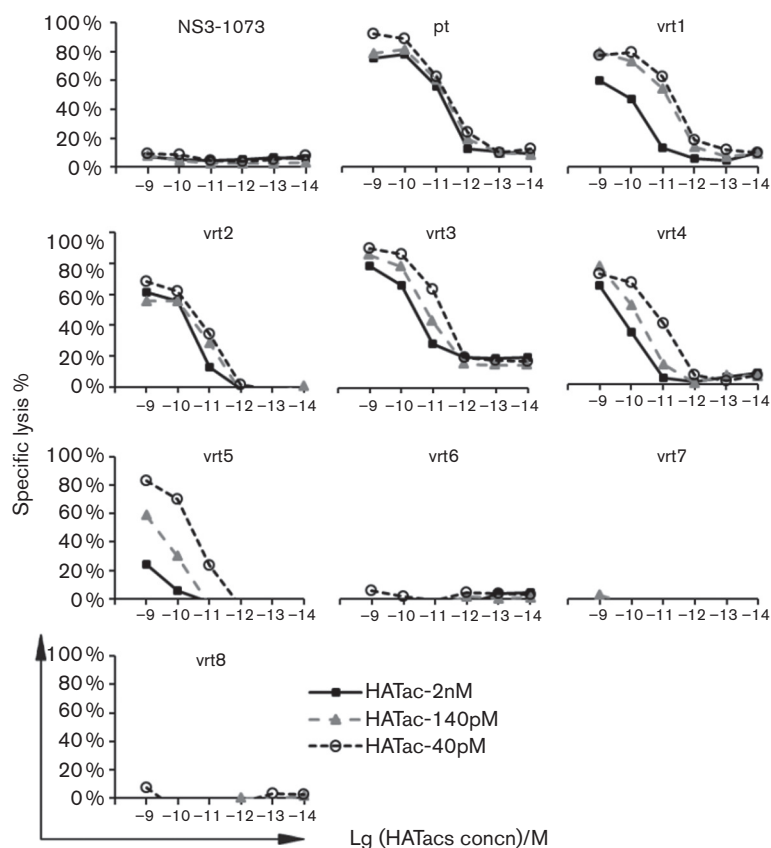


Fig. 5. Cytotoxicity assay with T2 cells loaded with mutant peptides. T2 cells were loaded with 2×10^{-6} M of control peptide or NS3-1406 peptides and then analysed as described in Fig. 4. Diagrams show the representative data of two repeated experiments.

reactive CD8⁺ T cell responses, especially none cross-reactive to genotype 1b variant (KLSALGLNAV). We have also found that, in other in-house studies, different TCRs against the same epitope can show distinct cross-reactivity patterns after affinity enhancement. Based on these studies, it is not difficult to predict that affinity enhancement for TCRs generated with antigen peptides such as genotype 1b variant (KLSALGLNAV) may result in HATs possessing wider cross-reactive attributes.

Previously, we enhanced the affinity of HIV gag-specific TCRs from 150 nM to 400 pM, and the HAT-transduced CD8⁺ T cells recognized and effectively killed HIV escape variants [23]. Here, we generated a series of NS3-1406 antigen-specific HATs [24, 25] with enhanced affinities from the original K_D of 6.6 μ M to 2 nM, 140 pM and even 40 pM. Additionally, we found that these HATs recognized the phylogenetically close mutant antigens, especially vrt1, with high affinity but showed relatively low affinity to the distant mutant antigens.

The HATac molecule is a class of soluble bispecific reagents with two binding moieties, one for pHLA (HAT) and one for CD3 (aCD3 scFv). The dissociation rate constants (k_d) and association rate constants (k_a) of the HAT moiety

change accordingly with variations of the peptides, but the aCD3 scFv moiety is constant for CD3 with a K_D of 44 nM, k_a of 4.35×10^4 ($M^{-1}s^{-1}$) and k_d of 1.61×10^{-3} (s^{-1}) (data not shown). Immune-mobilizing monoclonal TCRs against cancer (ImmTACs), which also possess the aCD3 scFv moiety, have been shown to mediate CTL killing, with the efficiency correlated with the strength of the TCR binding to pHLA [22]; however, the relations between k_a or k_d and CTL killing were not clear in that study. Interestingly, after analysing HATacs with K_D from 40 pM to 78 μ M for a group of pHLA antigens, we found that to effect minimal CTL killing, the k_a had to be at least 2.2×10^5 ($M^{-1}s^{-1}$), which was just five times higher than that of the aCD3 scFv binding to CD3. When k_a was 2.2×10^5 ($M^{-1}s^{-1}$), even with a k_d of 1.4×10^{-1} (s^{-1}) and K_D of 640 nM, which indicated about 20 times lower binding efficiency compared to the aCD3 scFv moiety binding to CD3, the HATac-140pM could still mediate CTL killing on cells presenting the vrt5 peptide antigen. In contrast, HATac-40pM, which bound pHLA-vrt6 with higher affinity of K_D at 410 nM, a k_d of 4.2×10^{-3} (s^{-1}) and k_a of 1.0×10^4 ($M^{-1}s^{-1}$), failed to mediate CTL killing on cells presenting the vrt6 peptide, indicating that a HATac could not activate CTLs if the k_a of its HAT for pHLA was weaker than that of the aCD3 scFv

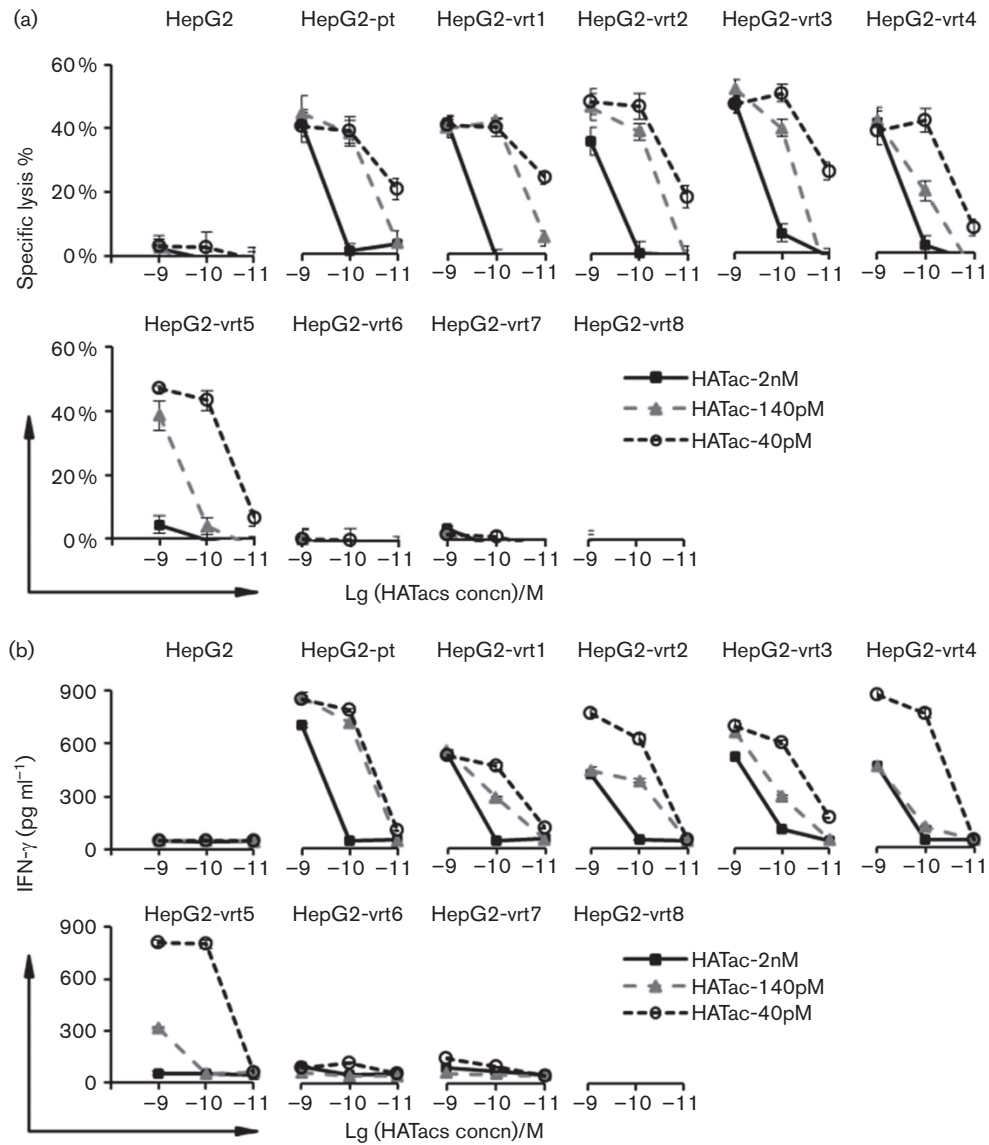


Fig. 6. Cytokine release and cytotoxicity assay with HepG2 cell lines expressing NS3-1406 antigens. HepG2 cells were engineered with lentiviral vectors to express truncated NS3-1406 antigens, which were fused with EGFP. The EGFP-positive cells were sorted by FACS. The cells were incubated with CD8⁺ T cells overnight in the presence of HATacs at the indicated concentrations. IFN-γ release (a) and specific lysis (b) were determined as in Fig. 4.

binding to CD3. Such a binding mode indicated that, in the most likely case, HATac binding to pHLA is completed before binding to CD3 on T cells.

HATac proteins, especially HATac-40pM, which could recognize several antigen mutants with high affinities and redirect CD8⁺ T cells to kill cells expressing these mutants, could provide a useful tool for eradicating HCV variants with escape mutations. Especially, directed molecular evolution might allow us to further improve the affinity of TCRs against phylogenetically distant mutants and generate new HATacs to capture a broad range of HCV escape variants. Importantly, during chronic infection, HCV-specific CTLs

go through the process of exhaustion and fail to eliminate infected cells. HATacs, the fusion proteins of HATs and αCD3 scFv, could redirect non-HCV-specific CTLs to recognize and kill both peptide-loaded T2 cells and HepG2 cells expressing escape mutants. Thus, the HCV antigen-specific T-cell exhaustion can be overcome by harnessing other specific CTLs with the application of HATac.

Pasetto *et al.* [31] proposed examining the possibility of adoptive T-cell immunotherapy using highly functional HCV-reactive T cells. Adoptive transfer of antigen-specific T lymphocytes, genetically engineered with antitumour TCRs, has emerged as an effective therapeutic strategy to

combat cancer [32]. Actually, adoptive transfer of virus-specific T cells was used in early-stage clinical trials for haematopoietic cell transplantation recipients to control infections such as those with Epstein–Barr virus [33], CMV [34], adenovirus [35] and polyomavirus JC [36], and showed low toxicity and long-term protection. However, the manufacturing processes to generate such engineered T cells for therapy, including isolation, activation, transduction and expansion, are expensive, labour intensive and time consuming. HATac could bind to target cells through the HAT moiety with high affinity up to pico-molar level and activate T cells through the anti-CD3 moiety, thus circumventing *in vitro* manipulations of T cells. Although early-stage clinical data from a recent study demonstrated potential therapeutic benefits in terms of a durable response and the ultimate breaking of T-cell tolerance via bi-functionally engineered HAT molecules [37], similar reagents have not been developed for virus control (by the time this manuscript had been prepared, similar molecules targeting HIV had been developed by Immunocore). In another study, an enhanced TCR (HAT) was produced for HIV gag-specific epitope SLYNTVATL (SL9), and CD8⁺ T cells transduced with the HAT suppressed HIV infection more effectively than cells transduced with natural SL9-specific TCR [23]. To the best of our knowledge, the present study is the first report of bi-functional T-cell activation molecules for HCV infections.

METHODS

Cell lines

Cell lines 293T and HepG2 were maintained in DMEM, and cell line T2 was maintained in Iscove's Modified Dulbecco's Medium (IMDM). All culture media were supplemented with 10% FBS, 100 U ml⁻¹ penicillin and 100 g ml⁻¹ streptomycin.

After each healthy donor had signed the written consent form, PBMCs were isolated from them with human Lymphoprep reagent (Axis-Shield), and CD8⁺ T cells were isolated from PBMCs with a human CD8⁺ T Cell Isolation Kit (Miltenyi Biotec) according to the manufacturer's protocol. To expand CD8⁺ T cells, 1 × 10⁶ CD8⁺ T cells were activated in a six-well plate with Human T-Activator CD3/CD28 Dynabeads (Life Technologies) at a bead-to-cell ratio of 1 : 1 in RPMI 1640 medium supplemented with 10% FBS, 100 U ml⁻¹ penicillin, 100 g ml⁻¹ streptomycin and 30 U ml⁻¹ recombinant human IL-2. An equal volume of fresh medium was added every 2 or 3 days, and after 7 or 8 days of activation from the start of the culture, CD8⁺ T cells were collected by removing the beads with a magnet.

To engineer HepG2 cells to express the NS3-1406 epitope, we transduced the cells using lentiviral vectors encoding a fusion gene of partial NS3 (amino acids 1353–1465) and the self-cleavage peptide 2A followed by EGFP. The partial NS3 gene was amplified from H/SG-Neo(L+I) plasmid (a kind gift from Professor Charles M. Rice [38]) with the primers NS3-f (5'-gagtagcatgGGCTCCGTCAGTGT-3') and NS3-r (5'-

gccggatccGCTGAAATCGACTGTCTGAG-3'). To construct the vectors expressing NS3-1406 mutants, a pair of reverse-complement primers (vrt-f and vrt-r) was synthesized covering the mutant sites, and the 5'-end and 3'-end of the partial gene were amplified with NS3-f/vrt-r and vrt-f/NS3-r, respectively, followed by overlapping with NS3-f/NS3-r. The recombinant vectors were co-transfected into 293T cells with packaging vectors pMD2.G, pRSV-REV and pMDLg/pRRE; HepG2 cells were infected with the virus-containing supernatant by centrifugation at 1000 g for 1 h at 32 °C. The EGFP-positive cells were sorted with a FACSAria II flow cytometer (BD Biosciences).

Protein expression and inclusion body purification

The pET-28a(+) vector or the modified vector with a biotinylation tag (LNDIFEAQKIEWH) at the C-terminus was used to express the codon-optimized genes coding the extracellular domains of the HLA-A0201 heavy chain (amino acids 25–300), the light chain β 2m, the TCR α and β chains, and CD3 γ or ϵ fusion proteins. All proteins were expressed as inclusion bodies (IBs) in *Escherichia coli* BL21 (DE3). To purify IB proteins, cells were collected by centrifugation at 8000 g for 10 min, and after washing with PBS, the cell pellet was resuspended with BugBuster Master Mix (Novagen, Merck Millipore) and stirred gently at room temperature for 20 min. IBs were spun down at 6000 g for 15 min and resuspended again with BugBuster Master Mix and stirred for another 5 min. Then, 30 ml of 10-fold diluted BugBuster was added and mixed, followed by centrifugation at 6000 g for 15 min. IBs were washed twice with 10-fold diluted BugBuster, and after rinsing with deionized water, the IBs were solubilized with the buffer containing 6 M guanidine/HCl, 50 mM Tris/Cl, 100 mM NaCl and 10 mM EDTA for further downstream processes.

pHLA preparation

The pHLA was refolded essentially as described by Garboczi *et al.* [39], with some modifications. Briefly, 1 mg peptide dissolved in DMSO was added to 40 ml stirred ice-cold refolding buffer (0.1 M Tris/HCl, 0.4 M L-arginine, 2 mM EDTA, 5 mM reduced glutathione, 0.5 mM oxidized glutathione and 0.2 mM PMSF, pH 8.3), followed by 1.2 mg HLA-A2 and 0.8 mg β 2m in 1 ml injection buffer (3 M guanidine/HCl, 10 mM sodium acetate, 10 mM EDTA, pH 4.2). HLA-A2 (1.2 mg) was added both 24 and 48 h later, and the refolding mixture was kept at 4 °C with gentle shaking for 3–4 days. At the end of refolding, the mixture was filtered through a 0.44 μ m membrane and then dialysed against 10 mM Tris/HCl (pH 8.0) in a 10 kDa cut-off tube at 4 °C for 24 h. The dialysed mixture was loaded onto a QHP column (GE Healthcare) equilibrated with 10 mM Tris/HCl (pH 8.0) and eluted with a linear gradient of NaCl with collection at 1.5 ml per fraction. The fractions with both HLA-A2 and β 2m were pooled and concentrated with a 10 kDa Amicon Ultra-15 Centrifugal Filter Unit (Amicon, Merck Millipore). The buffer for the pHLA not requiring biotinylation was changed to PBS in the filter unit, whereas that for the pHLA requiring biotinylation was changed to 10 mM

Tris/HCl (pH 8.0). BirA enzyme (Epigen Biotech) was used to biotinylate the tag of pHLA at 20 °C overnight. The reaction mixture was then diluted fivefold with 10 mM Tris/HCl (pH 8.0) and loaded again onto a QHP column to purify the pHLA_{bio}.

Phage display and HAT selections

The phage display libraries were constructed and screened as described previously [21]. Briefly, ν -genes of modified TCR α and β chains encoding a super-stable TCR variable domain (Y. Li, unpublished) were cloned into a phage display vector so that the V α and V β of the TCRs linked with the flexible linker GGGSEGGGGSEGGGGSEGGGSSE that was fused at the N-terminal of the phage coat protein III and displayed on the surface of filamentous bacteriophage M13. Then, mutations were introduced into CDR1 and CDR3 of TCR α and β chains by PCR to construct phagemid libraries that were electroporated into TG1 cells. After infection with KM13 helper phage and culturing the cells overnight at 30 °C in a flask with shaking, phage particles were purified by polyethylene glycol precipitation. To select phage particles displaying HATs, a process of bio-panning was performed with pHLA_{bio}-pt captured on streptavidin-coupled Dynabeads (Life Technologies), and then the phage particles were eluted and used to reinfect the TG1 cells. For screening of HATs at the end of three rounds of panning, phage particles from individual colonies were incubated with pHLA_{bio}-pt immobilized on streptavidin-coated 96-well plates, followed by detection with HRP-conjugated anti-M13 mAb (GE Healthcare).

Preparation of soluble TCR, HAT and HATac

The TCR α - and β -chain IBs were treated with 15 mM DTT at 37 °C for 30–45 min and then rapidly diluted into refolding buffer containing 5 M urea, 0.4 M L-arginine, 100 mM Tris/HCl (pH 8.0), 2 mM EDTA, 3.7 mM cystamine and 6.6 mM β -mercaptoethylamine. The refolding mixture was dialysed overnight against water and then twice against 10 mM Tris/HCl (pH 8.0). Soluble TCR was purified with anion exchange chromatography as above. HATs, whose β chains were fused with the biotin-tag, were further biotinylated and purified similarly as pHLA_{bio}. To purify HATacs, two consecutive rounds of anion exchange chromatography were used, i.e. the fractions from the first round were diluted fivefold with 10 mM Tris/HCl (pH 8.0) and reloaded onto the column, and the fractions from the second elution were pooled, concentrated and further purified with gel filtration. After endotoxin removal, the HATacs were aliquoted and stored at –80 °C. The CD3 was refolded, purified and biotinylated as HAT.

ELISA

ELISA strips were coated overnight at 4 °C with 100 μ l HATacs at 10 μ g ml^{–1} in PBS and blocked with PBS containing 5 % skim milk (PBSM) at room temperature for 1 h. Then, 100 μ l pHLA_{bio}-pt or biotinylated CD3 (CD3-bio) was added at 10 μ g ml^{–1} in PBSM and incubated for 1 h. After washing with PBS containing 0.05 % Tween 20

(PBST), 100 μ l HRP-conjugated streptavidin diluted 1 : 5000 in PBSM was added, and the strips were incubated for 20 min. The strips were then washed again with PBST and were developed with Tetramethylbenzidine (TMB) solution. After stopping with 1 M sulfuric acid, the strips were read at 450 nm with an ELISA plate reader. For long-washing ELISA, after incubation with pHLA_{bio}-pt, the strips were washed for the indicated times and immediately frozen at –80 °C until undergoing HRP-conjugated streptavidin incubation.

Cytotoxic assay

A CytoTox 96 Non-Radioactive Cytotoxicity Assay (Promega), which is based on LDH release, was used to measure cytotoxic lysis. The experiment was set up in 96-well U-bottom plates with RPMI 1640 medium without phenol red supplemented with 5 % FBS in a final volume of 200 μ l. Briefly, 4 \times 10⁴ T2 cells were loaded with peptides in 50 μ l for 2 h; then, 20 μ l HATacs was added at indicated concentrations, followed by 8 \times 10³ CD8⁺ T cells in 130 μ l volume. Plates were incubated for 20 h at 37 °C in a 5 % CO₂ incubator and then processed according to the instructions in the kit. The percentage of specific lysis was calculated using the following formula: (experimental well – control well without HATacs)/(target max – target spontaneous) \times 100 %.

SPR analysis

The affinity was determined by SPR BIAcore T200 (GE Healthcare). CM5 BIAcore chips were coated with streptavidin using amine coupling, and then biotinylated proteins were captured on the active channel. After blocking both the reference and active channels with 50 mM biotin, unbiotinylated proteins were injected sequentially through the reference and active channels at various concentrations with multi- or single-cycle kinetics. All measurements were performed at 25 °C. BIAcore T200 evaluation software was used to analyse the kinetic constants (k_a , k_d and K_D) with a 1 : 1 binding model.

Funding information

This study is supported by the Thousand Talent Program, Guangdong Province Leading Talent Program, the Guangdong Province Innovation Team Program (2013S047) and Innovation Commission Project Grants 201504010016.

Acknowledgements

We thank Hongwen Pang (Guangzhou Institutes of Biomedicine and Health) for technical help in anion exchange chromatography, Yi Zheng (Guangzhou Institutes of Biomedicine and Health) for help with flow cytometry and Dr Yung-Chun Hsu (XiangXue Life Sciences Research Center) for proofreading the manuscript.

Conflicts of interest

The authors declare that there are no conflicts of interest.

References

- Centers for Disease Control and Prevention. 2012. Hepatitis C information for the public. www.cdc.gov/hepatitis/C/cFAQ.htm#statistics.
- World Health Organization. Prevention & control of viral hepatitis infection: Framework for global action. World Health Organization; 2012.

3. Gogela NA, Lin MV, Wisocky JL, Chung RT. Enhancing our understanding of current therapies for hepatitis C virus (HCV). *Curr HIV/AIDS Rep* 2015;12:68–78.
4. Chayama K, Hayes CN. HCV drug resistance challenges in Japan: the role of pre-existing variants and emerging resistant strains in direct acting antiviral therapy. *Viruses* 2015;7:5328–5342.
5. Poveda E, Wyles DL, Mena A, Pedreira JD, Castro-Iglesias A et al. Update on hepatitis C virus resistance to direct-acting antiviral agents. *Antiviral Res* 2014;108:181–191.
6. Reherrmann B, Nascimbeni M. Immunology of hepatitis B virus and hepatitis C virus infection. *Nat Rev Immunol* 2005;5:215–229.
7. Thimme R, Oldach D, Chang KM, Steiger C, Ray SC et al. Determinants of viral clearance and persistence during acute hepatitis C virus infection. *J Exp Med* 2001;194:1395–1406.
8. Cox AL, Mosbruger T, Lauer GM, Pardoll D, Thomas DL et al. Comprehensive analyses of CD8+ T cell responses during longitudinal study of acute human hepatitis C. *Hepatology* 2005;42:104–112.
9. Cox AL, Mosbruger T, Mao Q, Liu Z, Wang XH et al. Cellular immune selection with hepatitis C virus persistence in humans. *J Exp Med* 2005;201:1741–1752.
10. Merani S, Petrovic D, James I, Chopra A, Cooper D et al. Effect of immune pressure on Hepatitis C virus evolution: insights from a single-source outbreak. *Hepatology* 2011;53:396–405.
11. Tester I, Smyk-Pearson S, Wang P, Wertheimer A, Yao E et al. Immune evasion versus recovery after acute hepatitis C virus infection from a shared source. *J Exp Med* 2005;201:1725–1731.
12. Ulsenheimer A, Paranhos-Baccalà G, Komurian-Pradel F, Raziorrouh B, Kurktschiev P et al. Lack of variant specific CD8+ T-cell response against mutant and pre-existing variants leads to outgrowth of particular clones in acute hepatitis C. *Viral J* 2013;10:295.
13. Wölfel M, Rutebemberwa A, Mosbruger T, Mao Q, Li HM et al. Hepatitis C virus immune escape via exploitation of a hole in the T cell repertoire. *J Immunol* 2008;181:6435–6446.
14. Klenerman P, Thimme R. T cell responses in hepatitis C: the good, the bad and the unconventional. *Gut* 2012;61:1226–1234.
15. Wherry EJ. T cell exhaustion. *Nat Immunol* 2011;12:492–499.
16. Bensch B, Seigel B, Ruhl M, Timm J, Kuntz M et al. Coexpression of PD-1, 2B4, CD160 and KLRG1 on exhausted HCV-specific CD8+ T cells is linked to antigen recognition and T cell differentiation. *PLoS Pathog* 2010;6:e1000947.
17. Nitschke K, Flecken T, Schmidt J, Gostick E, Marget M et al. Tetramer enrichment reveals the presence of phenotypically diverse hepatitis C virus-specific CD8+ T cells in chronic infection. *J Virol* 2015;89:25–34.
18. Penna A, Pilli M, Zerbini A, Orlandini A, Mezzadri S et al. Dysfunction and functional restoration of HCV-specific CD8 responses in chronic hepatitis C virus infection. *Hepatology* 2007;45:588–601.
19. Dustin ML, Depoix D. New insights into the T cell synapse from single molecule techniques. *Nat Rev Immunol* 2011;11:672–684.
20. Manz BN, Jackson BL, Petit RS, Dustin ML, Groves J. T-cell triggering thresholds are modulated by the number of antigen within individual T-cell receptor clusters. *Proc Natl Acad Sci USA* 2011;108:9089–9094.
21. Li Y, Moysey R, Molloy PE, Vuidepot AL, Mahon T et al. Directed evolution of human T-cell receptors with picomolar affinities by phage display. *Nat Biotechnol* 2005;23:349–354.
22. Liddy N, Bossi G, Adams KJ, Lissina A, Mahon TM et al. Monoclonal TCR-redirectioned tumor cell killing. *Nat Med* 2012;18:980–987.
23. Varela-Rohena A, Molloy PE, Dunn SM, Li Y, Suhoski MM et al. Control of HIV-1 immune escape by CD8 T cells expressing enhanced T-cell receptor. *Nat Med* 2008;14:1390–1395.
24. Callender GG, Rosen HR, Roszkowski JJ, Lyons GE, Li M et al. Identification of a hepatitis C virus-reactive T cell receptor that does not require CD8 for target cell recognition. *Hepatology* 2006;43:973–981.
25. Rosen HR, Hinrichs DJ, Leistikow RL, Callender G, Wertheimer AM et al. Cutting edge: identification of hepatitis C virus-specific CD8+ T cells restricted by donor HLA alleles following liver transplantation. *J Immunol* 2004;173:5355–5359.
26. Boulter JM, Glick M, Todorov PT, Baston E, Sami M et al. Stable, soluble T-cell receptor molecules for crystallization and therapeutics. *Protein Eng* 2003;16:707–711.
27. Cole DK, Pumphrey NJ, Boulter JM, Sami M, Bell JI et al. Human TCR-binding affinity is governed by MHC class restriction. *J Immunol* 2007;178:5727–5734.
28. Timm J, Walker CM. Mutational escape of CD8+ T cell epitopes: implications for prevention and therapy of persistent hepatitis virus infections. *Med Microbiol Immunol* 2015;204:29–38.
29. Giugliano S, Oezkan F, Bedrejowski M, Kudla M, Reiser M et al. Degree of cross-genotype reactivity of hepatitis C virus-specific CD8+ T cells directed against NS3. *Hepatology* 2009;50:707–716.
30. Ziegler S, Skibbe K, Walker A, Ke X, Heinemann FM et al. Impact of sequence variation in a dominant HLA-A*02-restricted epitope in Hepatitis C virus on priming and cross-reactivity of CD8+ T cells. *J Virol* 2014;88:11080–11090.
31. Pasetto A, Aleman S, Chen M. Functional attributes of responding T cells in HCV infection: the recent advances in engineering functional antiviral T cells. *Arch Immunol Ther Exp* 2014;62:23–30.
32. Rosenberg SA, Restifo NP. Adoptive cell transfer as personalized immunotherapy for human cancer. *Science* 2015;348:62–68.
33. Heslop HE, Slobod KS, Pule MA, Hale GA, Rousseau A et al. Long-term outcome of EBV-specific T-cell infusions to prevent or treat EBV-related lymphoproliferative disease in transplant recipients. *Blood* 2010;115:925–935.
34. Walter EA, Greenberg PD, Gilbert MJ, Finch RJ, Watanabe KS et al. Reconstitution of cellular immunity against cytomegalovirus in recipients of allogeneic bone marrow by transfer of T-cell clones from the donor. *N Engl J Med* 1995;333:1038–1044.
35. Feuchtinger T, Matthes-Martin S, Richard C, Lion T, Fuhrer M et al. Safe adoptive transfer of virus-specific T-cell immunity for the treatment of systemic adenovirus infection after allogeneic stem cell transplantation. *Br J Haematol* 2006;134:64–76.
36. Balduzzi A, Lucchini G, Hirsch HH, Basso S, Cioni M et al. Polyomavirus JC-targeted T-cell therapy for progressive multiple leukoencephalopathy in a hematopoietic cell transplantation recipient. *Bone Marrow Transplant* 2011;46:987–992.
37. Oates J, Hassan NJ, Jakobsen BK. ImmTACs for targeted cancer therapy: why, what, how, and which. *Mol Immunol* 2015;67:67–74.
38. Blight KJ, Mckeating JA, Marcotrigiano J, Rice CM. Efficient replication of hepatitis C virus genotype 1a RNAs in cell culture. *J Virol* 2003;77:3181–3190.
39. Garboczi DN, Hung DT, Wiley DC. HLA-A2-peptide complexes: refolding and crystallization of molecules expressed in *Escherichia coli* and complexed with single antigenic peptides. *Proc Natl Acad Sci USA* 1992;89:3429–3433.